



Genome-wide genetic variations are highly correlated with proximal DNA methylation patterns.

Shinichi Morishita, Wei Qu, Shin-ichi Hashimoto, et al.

Genome Res. published online June 11, 2012

Access the most recent version at doi:[10.1101/gr.140236.112](https://doi.org/10.1101/gr.140236.112)

P<P	Published online June 11, 2012 in advance of the print journal.
Accepted Manuscript	Peer-reviewed and accepted for publication but not copyedited or typeset; accepted manuscript is likely to differ from the final, published version.
Open Access	Freely available online through the <i>Genome Research</i> Open Access option.
Creative Commons License	This manuscript is Open Access. This article is distributed exclusively by Cold Spring Harbor Laboratory Press for the first six months after the full-issue publication date (see http://genome.cshlp.org/site/misc/terms.xhtml). After six months, it is available under a Creative Commons License (Attribution-NonCommercial 3.0 Unported License), as described at http://creativecommons.org/licenses/by-nc/3.0/ .
Email Alerting Service	Receive free email alerts when new articles cite this article - sign up in the box at the top right corner of the article or click here .



To subscribe to *Genome Research* go to:
<https://genome.cshlp.org/subscriptions>

Genome-wide genetic variations are highly correlated with proximal DNA methylation patterns.

Wei Qu^{1,*}, Shin-ichi Hashimoto¹, Atsuko Shimada², Yoichiro Nakatani¹, Taro L Saito¹, Katsumi Ogoshi³, Kouji Matsushima³, Yutaka Suzuki⁴, Sumio Sugano⁴, Hiroyuki Takeda², and Shinichi Morishita^{1,*}

1 Department of Computational Biology, Graduate School of Frontier Sciences, The University of Tokyo, Kashiwa 277-0882, Japan.

2 Department of Biological Sciences, Graduate School of Science, The University of Tokyo, Tokyo 113-0033, Japan.

3 Department of Molecular Preventive Medicine, Graduate School of Medicine, The University of Tokyo, Tokyo 113-0033.

4 Department of Medical Genome Sciences, Graduate School of Frontier Sciences, The University of Tokyo, Tokyo 108-8639, Japan.

* joint corresponding authors

Abstract

5-methyl-cytosines at CpG sites frequently mutate into thymines, accounting for a large proportion of spontaneous point mutations. The repair system would leave substantial numbers of errors in neighboring regions if the synthesis of erased gaps around deaminated 5-methyl-cytosines is error-prone. Indeed, we identified an unexpected genome-wide role of the CpG methylation state as a major determinant of proximal natural genetic variation. Specifically, 507 Mbp (~18%) of the human genome was within 10 bp of a CpG site; in these regions, the single nucleotide polymorphism (SNP) rate significantly increased by ~50% ($p < 10^{-566}$ by two-proportion z-test) if the neighboring CpG sites are methylated. To reconfirm this finding in another vertebrate, we compared six single-base resolution methylomes in two inbred medaka (*Oryzias latipes*) strains with sufficient genetic divergence (3.4%). We found that the SNP rate also increased by ~50% ($p < 10^{-2170}$) and the substitution rates in all dinucleotides increased simultaneously ($p < 10^{-441}$) around methylated CpG sites. In the hypomethylated regions, the “CGCG” motif was significantly enriched ($p < 10^{-680}$) and evolutionarily conserved ($p = \sim 0.203\%$), and slow CpG deamination rather than fast CpG gain was seen, indicating a possible role of CGCG as a candidate *cis*-element for the hypomethylation state. In regions that were hypermethylated in germline-like tissues but were hypomethylated in somatic liver cells, the SNP rate was significantly smaller than that in hypomethylated regions in both tissues, suggesting a positive selective pressure during DNA methylation reprogramming. This is the first report of findings showing that the CpG methylation state is significantly correlated with the characteristics of evolutionary change in neighboring DNA.

Introduction

Our understanding of the role of DNA methylation in genetic variation is limited to the observation that methylated cytosines at CpG sites mutate to thymines at very high frequencies (Lindahl and Nyberg 1972; Coulondre et al. 1978; Cooper and Krawczak 1989). This has been confirmed in genome-wide analyses (Sved and Bird 1990; Lander et al. 2001; Venter et al. 2001). Recently, precise methylation maps at single-base resolution have been created using next-generation DNA sequencing technology, confirming the overabundance of G:C→A:T transitions (Ossowski et al. 2010). In contrast, hypomethylated cytosine nucleotides seem to escape mutation; *e.g.*, comparative genome analysis of human and primates genomes showed a lower CpG mutation rate in CpG-rich promoters that are mostly hypomethylated in the germline (Saxonov et al. 2006; Weber et al. 2007). Although the system for repairing mutations of 5-methyl cytosines to thymines is not well understood, it must be relatively ineffective because a large proportion of spontaneous point mutations are C-to-T mutations. The erroneous repair system may also leave substantial errors in neighboring regions if the synthesis of erased gaps around deaminated 5-methyl-cytosines is error-prone. The genome-wide methylation information provides an unprecedented opportunity to examine whether the CpG methylation state affects proximal genetic variation.

A related problem is the allele-specific DNA methylation (ASM), different methylation patterns in parental alleles (Chandler et al. 1987). ASM is involved in genomic imprinting and X-inactivation in females to achieve dosage compensation. Autosomal ASM has been also reported in the human and mouse genomes (Yamada et al. 2004; Heijmans et al. 2007; Zhang et al. 2009), and recent genome-wide collections of DNA methylation state have started uncovering that ASM is prevalent in the mammalian genome (Kerkel et al. 2008; Hellman and Chess 2010; Schalkwyk et al. 2010). Genome-wide studies indicate that ASM is associated with *cis*-acting polymorphisms (local genotypes), such as mutations

in CpG sites (Schilling et al. 2009; Shoemaker et al. 2010a), suggesting Mendelian inheritance patterns of ASM. A number of genomic regions of intermediate DNA methylation level are found in the human genome (Deng et al. 2009; Lister et al. 2009) and are thought to be largely a consequence of ASM and have implications for complex disease genetics (Meaburn et al. 2010). Little is, however, known about fundamental *cis*-elements for inducing DNA methylation. Sequence motifs that are significantly enriched and evolutionarily conserved in hypomethylated regions could be candidate *cis*-elements; however, it is highly non-trivial to identify conserved sequence motifs due to the quite low incidence of genetic variation (~0.1%) in the human and mouse genomes. We approach this problem through the study of correlation between CpG methylation state and proximal genetic variation in the medaka genome.

Results

We examined the relationship between DNA methylation and genetic variation in the human genome using publicly available data. Specifically, we examined the methylome data from human germline sperm cells (Molaro et al. 2011), and the reference single nucleotide polymorphisms (refSNPs) of the CEU population collected by the HapMap Project (International 2003). Although substantial data are available on the human genome, the incidence of genetic variation in the human genome is quite low (~0.1%), which is not sufficient to perform a detailed analysis on the dinucleotide patterns of genetic variations associated with hyper- and hypomethylated regions. For this purpose, the medaka (*Oryzias latipes*) model system provides an ideal resource in vertebrates because two medaka inbred strains, Hd-rR and HNI, have a sufficiently high incidence of genetic variation (~3.4%) (Kasahara et al. 2007). The Hd-rR and HNI medaka inbred strains originated in the southern and northern parts of Japan, respectively, which were separated by a watershed, and the strains diverged approximately 18 million years ago (Setiamarga et al. 2009). Another merit of the medaka is its abundance of germline cells

in the testes and blastulae [half-day embryos, in which some of cells remain totipotent (Hong et al. 1998)], which provides information on the primary relationships between the methylation pattern and genomic variation during the course of evolution. Thus, we newly generated six methylomes of medaka genomes at single-base resolution using genomic DNA from three libraries (liver, blastulae, and testes) of the two strains, treating it with bisulphite, and subjecting it to Illumina sequencing. In total, 1.8 billion reads were produced and 44 billion nucleotides were uniquely mapped to the genome, with an average depth of nine fold for each cell line of each strain (Table S1). An average of ~78% of each medaka genome was covered by at least one read (Table S1). The bisulphite conversion procedure was highly effective, as validated by a control experiment using yeast (*Saccharomyces cerevisiae* S288C) (Table S2). In yeast, cytosine nucleotides are not methylated, and indeed, none of yeast cytosine nucleotides was uncovered to be hypermethylated (methylation level ≥ 0.8 , Fig. S1). Data for the entire methylome of medaka at single base resolution can be accessed at <http://utgenome.org/medaka/methylome/>.

Substantial cytosines at non-CpG sites are methylated in human ES and *Arabidopsis* (Cokus et al. 2008; Lister et al. 2008; Lister et al. 2009); however, methylation at non-CpG sites was very rare in human sperm (Molaro et al. 2011) and in all of the three medaka tissues (Fig. S2); i.e., few non-CpG cytosines (~0.02%) were observed to be hypermethylated. To examine whether cytosine methylation state, unmethylated or methylated, affects proximal genetic variation, both of unmethylated and methylated cytosines should be sufficiently available. In CpG sites, the ratio of unmethylated cytosines : methylated cytosines was ~10% : ~90%, showing the abundance of unmethylated cytosines. In non-CpG sites, however, the ratio was 99.98% : 0.02%, indicating the lack of methylated cytosines. Thus, we focused on methylation patterns of CpG sites in subsequent analyses. The distribution of methylation levels was found to be bimodal, and the vast majority of CpG sites

were highly methylated in human sperm (Molaro et al. 2011) and in each medaka library (Fig. S2). CpG islands may be appropriate regions in which to measure the effect of methylation pattern on the incidence of genetic variation; however, they occupy a relatively small proportion of the human genome (~1%) as well as the medaka genome (~3%) and exist mostly in CpG-rich regions. Therefore, regions with fewer CpG sites are overlooked. For defining more comprehensive characteristics of CpG sites in a wider range of genome sequences, we instead focused on neighboring genome sequences (the 10 bases upstream and downstream) of all the CpG sites, which we hereafter refer to as “CpG site blocks” (see Methods and Table S3). Overlapping CpG site blocks were merged, and the combined length of all the CpG site blocks was 507 Mbp (~18%) in the human genome and ~188 Mbp in the medaka genome, accounting for ~37% of the ~500 Mbp that were aligned between the two medaka genomes. We then noticed that one third of CpG site blocks were covered by <5 reads and were likely to lack accuracy. Thus, we imposed the stringent requirement that each CpG site had a read coverage of ≥ 5 (see Methods). CpG site blocks that met this condition accounted for ~323 Mbp (~11%) in the human genome and ~139 Mbp (~28%) in the medaka genome, which was sufficient for estimating features of the entire genomes (Table S3).

We compared the incidence of genetic variations in hypomethylated regions (methylation level ≤ 0.2) with that in hypermethylated regions (methylation level ≥ 0.8). Because single-nucleotide mutations by deamination of methylated cytosines in CpG dinucleotides are dominant, to examine single-nucleotide substitution rates in this analysis, we excluded SNPs in CpG dinucleotides and SNPs in TpG/CpA dinucleotides which might make TpG/CpA be CpG. Fig. 1A shows that, in human sperm, the incidence rate in hypomethylated regions in entire genome, 0.054%, was significantly lower than that in hypermethylated ones, 0.081% ($p < 10^{-566}$ by two-proportion z -test, Table S4). This significant increase of incidence rate in hypermethylated regions were also detected in intergenic regions ($p < 10^{-305}$), in exons ($p < 10^{-29}$), and in introns ($p <$

10^{-151} , Table S4). We also observed a similar tendency in the medaka system. For example, Fig. 1B illustrates a pair of the homologous regions of the human and medaka genomes where RPS13 gene is encoded. We saw four SNPs in the hypermethylated human region and a higher SNP rate in the hypermethylated medaka region. We will check this characteristic precisely in the entire medaka genome in what follows.

In medaka, the methylation state of each CpG site is not necessarily conserved between the two strains (Fig. 1C and 1D, Table S3A), which is supported by 4.46×10^{-4} methylation polymorphisms per CG site per generation in *Arabidopsis thaliana* (Schmitz et al. 2011). In general, however, hypomethylated and hypermethylated regions were highly conserved between the two inbred strains (Fig. 1C and 1D) and were also highly correlated ($R^2 = 0.73$) between testes and blastulae (Fig. 1E). Thus, hereafter, we used hypo- and hypermethylated regions that were conserved between the two strains as the representative regions. Analysis of SNPs between Hd-rR and HNI (Sasaki et al. 2009) around CpG blocks revealed that the SNP rate of 1.81% in hypomethylated regions was significantly lower than the 2.78% rate in hypermethylated regions (Fig. 1F, $p < 10^{-2170}$ by two-proportion z -test, Table S4). In addition to the entire genome, these characteristics were also significant in intergenic regions ($p < 10^{-2170}$), in introns ($p < 10^{-589}$), and in exons ($p < 10^{-113}$) despite of inherently strong purifying selection in exons (Fig. 1F, Table S4). Furthermore, genome-wide regions that were differentially methylated in the two strains exhibited a SNP rate of 3.41%, which is significantly higher than the rate of 2.78% in hyper-methylated regions ($p < 10^{-442}$, Table S4). This indicates that genomic regions with a relaxed selective pressure display a wider divergence in cytosine methylation.

The high divergence between the two medaka strains provided a detailed analysis on mutations of dinucleotides. Fig. 1G

shows that the peak substitution rates occurred in CG and TA dinucleotides. The CG substitutions (~11% in hypermethylated regions) were predominantly transitions, which can be explained by the deamination of methylated cytosines that dominates point substitutions in vertebrates (Lindahl and Nyberg 1972; Cooper and Krawczak 1989), whereas in hypomethylated regions, the CG substitution rate was moderate. Another commonly mutated dinucleotide, TA, is universally underrepresented because of its high mutation rate (Ohno 1988; Burge et al. 1992). Our novel finding is that substitution rates for all dinucleotides in CpG site blocks change simultaneously when neighboring CG dinucleotides are hypermethylated, hypomethylated, or differentially methylated. These characteristics were significant for any dinucleotide in the entire genome ($p < 10^{-441}$ by two proportion z -test), in intergenic regions ($p < 10^{-263}$), in introns ($p < 10^{-69}$), and in exons ($p < 10^{-15}$), implying that methylation patterns have a comprehensive impact on genetic variation (see the p -values for all dinucleotides in Table S5).

One might be concerned that the high CG substitution rate could affect the substitution rates for dinucleotides other than CG; however, the effects are limited to dinucleotides immediately before CG dinucleotides and are considerably small due to the rarity of CG dinucleotides (2.0% in the medaka genome). In fact, the substitution rates of dinucleotides excluding the dinucleotides overlapping CGs by one base remain essentially unchanged (Fig. S3). Another possible explanation for the slower mutation rate in evolutionarily conserved hypomethylated regions is that these regions are around transcription start site (TSS) regions that are high conserved (Taylor et al. 2006; Sasaki et al. 2009); however, evolution in such regions remained approximately the same even after hypomethylated regions near TSSs (those lying in the 500 bp immediately upstream and downstream of the TSSs for 23,531 predicted medaka genes) were excluded from the analysis (Fig. S4, Table S3A and S3B). The higher substitution rate in evolutionarily conserved hypermethylated regions may be influenced by

transposable elements which are highly mutated and methylated in vertebrates (Goll and Bestor 2005). However, transposons in the medaka genome are extremely rare and can be ignored (Kasahara et al. 2007). Therefore, methylation-dependent factors other than the influence by gene transcription or transposons may contribute to the slow evolution of hypomethylated regions.

A related problem is that methylation patterns may be affected by *cis*-acting polymorphisms, such as mutations in CpG sites (Schilling et al. 2009; Shoemaker et al. 2010b), but little is known about fundamental *cis*-elements. It is highly nontrivial to identify *cis*-elements that induce CpG methylation state. We attempted to find sequence motifs that were enriched and evolutionarily conserved in hypomethylated regions because such motifs could be candidate *cis*-elements and would be informative for further studies. We therefore searched for potential conserved motifs that were capable of distinguishing two collections of 10,000 hypo- or hypermethylated CpG site blocks using AdaBoost, an established machine learning algorithm (see Methods). The most significant motif was “CGCG,” and the incidence of “CGCG” in 10,000 hypomethylated regions was 61.39%, compared with 21.84% in 10,000 hypermethylated regions, showing the significant relevance of “CGCG” sequence enrichment to the methylation state ($p < 10^{-680}$ by two-proportion *z*-test), as illustrated in Fig. 2A. We then examined whether the CGCG motif is evolutionarily conserved in hypomethylated regions. For this purpose, it was necessary to predict the ancestor of Hd-rR and HNI strains. Therefore, we assembled a draft genome of an outgroup medaka strain, HSOK. Fig. 2B shows that CGCG is significantly more conserved in hypomethylated regions than in hypermethylated regions ($p = \sim 0.203\%$ by two-proportion *z*-test). This evolutionarily preserved CGCG motif in hypomethylated regions may be attributable to slow CpG deamination or fast CpG-gaining. To clarify this issue, we calculated dinucleotide-gaining substitution rates by comparing the genomes of Hd-rR and HNI to their ancestor which was

estimated from the outgroup HSOK genome (Fig. 2C, see Methods). The rate of CpG gain in hypomethylated regions, 1.4%, was much smaller than the 3.0% rate observed in hypermethylated ones, supporting the hypothesis that slow CpG deamination is the dominant factor for maintaining CGCG richness in hypomethylated regions (Cohen et al. 2011). Meanwhile, we observed an intriguing property in differentially methylated regions in different strains: the rates of CG/CC gain in the hypomethylated mate are higher than those in the hypermethylated mate (3.3% and 2.4% compared with 2.6% and 2.2%, respectively), suggesting that CG/CC gains are involved in the evolution of methylation among different strains.

Next we examined the methylation and genetic variations of two germline-like tissue types (blastulae and testes) and somatic liver cells that are fully differentiated and mostly homogeneous. In this analysis, we focused on tissue types in a single strain, Hd-rR. Fig. 3A shows an abundance of CpG cite blocks with tissue-differentially methylation states such that differences in methylation levels between each of germ-line-like tissues and liver are more than 0.5. Notably, ~99% of tissue-differentially-methylated regions were hypomethylated in the liver but were hypermethylated in blastulae and testes. Remarkably, as illustrated in Fig. 3B, the tissue-differentially-methylated regions showed a significantly lower SNP rate than did the hypomethylated ones ($p < 10^{-82}$, Table S6). Further analysis on dinucleotides revealed that the substitution rates of dinucleotides except for CC/GG/CG in differentially methylated regions were also significantly lower than were those in hypomethylated regions (Fig. 3C, $p < 10^{-3}$, Table S7A), which was also seen even after excluding regions near TSSs (Fig. S6). The high CG substitution rate in these regions could have been a consequence of deamination mutations occurring in primary germ-line-like cells. These results suggest that, because change in DNA methylation can affect transcription so that it can regulate reprogramming during somatic development, a positive selective pressure of genomic sequence could be involved in these differentially methylated regions (Fig. 3D).

Discussion

Because DNA methylation may influence genetic variation, we measured the incidence of genetic variations in methylation states in the human genome as well as in the two medaka inbred strains. We focused on germ-line-like tissue types, blastulae and testes, to determine the primary effects of methylation and evaluated a total of six single-base-resolution DNA methylomes in the medaka system. Our findings provide novel insights into the relationships between the dynamics of methylation states and genomic variations (Fig. 2A and Fig. 3D). Fig. 4 illustrates our hypothesis for explaining the difference observed in genetic evolution between hyper- and hypomethylated region. Given that deaminated cytosine (U:G mismatch) is recognized and repaired by base excision repair (BER), deaminated 5-methyl-cytosine (T:G mismatch) would be corrected via more complicated mismatch-repair pathways (Molaro et al. 2011) (Fig. 4). Previous studies revealed that two glycosylases, thymine DNA glycosylase (TDG) and methyl-CpG-binding domain protein 4 (MBD4), are associated with T:G repair, but processing by these enzymes is biased in the genome and is relatively ineffective (Neddermann et al. 1996; Yoon et al. 2003). An alternative mismatch-repair system (MMR) might gain access to T:G mismatches, which could involve DNA polymerases with lower fidelity (Loeb and Monnat 2008). Thus, we speculate that the error-prone synthesis of the erased gaps around deaminated 5-methyl-cytosines could lead to a higher mutation rate in hypermethylated regions (Fig. 4).

In an effort of searching for candidate *cis*-elements of affecting CpG methylation state, we observed a significant correlation between the methylation state of CpG sites and the presence of CGCG in neighborhood. This CGCG motif was evolutionarily conserved in hypomethylated regions with a statistical significance. A comparative genomic analysis showed

slow CpG-gaining in hypomethylated regions, supporting the hypothesis that the evolutionary conservation of CGCG was brought about by slow CpG deamination (Cohen et al. 2011). It is intriguing to ask whether or not CGCG and other candidate motifs are associated with or affect allele-specific methylation. Breeding the F1 generation of the two medaka inbred strains is a promising approach to this problem, and high-throughput short read bisulfite sequencing is an inexpensive way of observing DNA methylome, though it suffers from the technical difficulty in distinguishing short reads of ~100bp from two different alleles. The high incidence of genetic variation (~3.4%) between the two inbred strains would facilitate achieving this classification task because an average of 3.4 SNPs per 100bp read would make it easier to align a read to its originating allele.

Overall, these genetic consequences of methylation, including the slower evolution rate of the *cis*-element “CGCG” found in hypomethylated regions of the medaka system, should be also explored in other species.

Methods

Construction and Sequencing of Medaka Bisulfite-treated DNA Libraries

Genomic DNA from medaka tissue cells (blastulae, testes and liver from two medaka strain, Hd-rR and HNI) was isolated and sonicated to a desired size range (100 – 400 bp). The DNA fragments were treated with DNA polymerase to generate blunt end, and were ligated with double-stranded DNA adaptors containing methylated cytosines, which were designed to amplify only those DNA fragments carrying bisulfite-converted adaptor sequences at both ends. Followed by 7~10 cycles of PCR, 250 ~450bp size-fractionated DNA was sequenced using an Illumina GAIIx genome analyzer. A validation experiment was performed according to the same procedure using genomic DNA from *Saccharomyces cerevisiae* S288C.

Computational and Statistical Methods

We converted all cytosines in reads and in both the Watson and Crick strands of the reference genome to thymines for primary mapping, and used Smith-Waterman alignments between the original sequences of primary best hits. All possible methylation patterns were evaluated and only uniquely mapped reads were retained for further analyses. The level of methylation of a particular cytosine was estimated by dividing the number of mapped reads reporting a cytosine (C) by the total number of reads reporting a C or T (thymine). The comparison of substitution rate and methylation level was performed among CpG site blocks, which consist of at least one CpG site and its surrounding upstream or downstream ten bases. Overlapping CpG site blocks were merged. Two proportion z-test was performed to test the significance of substitution rate difference observed between hypo-/hypermethylated CpG site blocks. The AdaBoost algorithm was used to find conserved motifs in hypo-/hypermethylated CpG site blocks. Estimation of the ancestor sequence of Hd-rR and HNI was given by multiple alignments using an out-group medaka strain HSOK which was assembled using the SOAP de novo assembler (Li et al. 2010). Details of Methods could be found in Supplemental Materials and Methods.

Data Access All sequence data are deposited at the NCBI Archive (accession number SRA026693).

Acknowledgements

This work was supported in part by a Grant-in-Aid for Scientific Research (A, 23241058) from the MEXT, by the Global COE program (Deciphering Biosphere from Genome Big Bang) from the MEXT, and by the Innovative Cell Biology by Innovative Technology from the MEXT. Computational time was provided by the Information Technology Center, the University of Tokyo.

Figure legends

Figure 1. Methylation patterns and substitution rates in the inbred medaka strains, Hd-rR and HNI. **(A)** SNP (single-nucleotide polymorphism) rates in hyper- and hypomethylated CpG blocks in the reference human genome (hg19). The difference in SNP rates was significant in the entire genome ($p < 10^{-566}$ by two-proportion z -test, Table S4), in intergenic regions ($p < 10^{-305}$), in exons ($p < 10^{-29}$), and in introns ($p < 10^{-151}$). **(B)** Methylation level and SNP distribution in the homologous regions of the human and medaka genomes where gene RPS13 is coded. **(C-D)** Comparisons of the methylation patterns in Hd-rR and HNI. The vertical and horizontal axes indicate methylation level. The heat map uses logarithmic coordinates and presents the number of corresponding CpG site blocks. Conserved hypermethylated and hypomethylated patterns between the two strains were dominant, except for a small number of hot spots observed in the differentially methylated regions (differences in methylation level ≥ 0.5). **(E)** Comparison of the methylation patterns in blastulae and testes in Hd-rR. **(F)** SNP rates in hypo-, hyper-, and strain-differentially-methylated regions in medaka blastulae grouped by the entire genome, intergenic regions, exons, and introns. The differences between SNP rates of hypo- and hypermethylated regions were remarkable: $p < 10^{-2170}$ (genome), $p < 10^{-2170}$ (intergenic regions), $p < 10^{-113}$ (exons), and $p < 10^{-589}$ (introns) according to two-proportion z -test (Table S4). Furthermore, the differences between SNP rates of strain-differentially- and hypermethylated regions were also significant (Table S4). **(G)** Dinucleotide substitution rates in the whole medaka genome, intergenic regions, exons and introns in CpG site blocks with various methylation states. Color key presents mutation rates: blue for hypermethylated (methylation level ≥ 0.8 in both strains); red for hypomethylated (methylation level ≤ 0.2 in both strains); and green for strain-differentially methylated (difference in methylation level between the two strains ≥ 0.5) in blastulae. The axes in each radar chart represent substitution rates of individual dinucleotides. Each dinucleotide shows the same substitution rate as its reverse complementary dinucleotide. Significant

differences between substitution rates in hypo- and hypermethylated regions were observed for all dinucleotides, and the p -values according to two-proportion z -test were $p < 10^{-441}$ (genome), $p < 10^{-263}$ (intergenic regions), $p < 10^{-15}$ (exons), and $p < 10^{-69}$ (introns) (Table S5).

Figure 2. (A) Representative mutation patterns in evolutionarily conserved hypo- and hypermethylated regions and in regions that are differentially methylated in different strains, where substitution rates ascend from top to bottom. CGCG motif is significantly conserved in hypomethylated regions ($p < 10^{-680}$ by two proportion z -test). (B) Number of strain-differentially methylated CpG site blocks with either gain or loss of the CGCG motif. Of 1,656 CGCG motif occurrences in multiple alignments of the genomes of the three strains, 52 (24, respectively) were conserved in hypomethylated (hypermethylated) regions of one of Hd-rR or HNI but were mutated in hypermethylated (hypomethylated) regions of the other strain. We then evaluated the significance of the difference between the means in the two groups, 52/1656 vs. 24/1656, to obtain a p -value of 0.203% according to a two-proportion z -test. (C) The rates of dinucleotide gain in CpG site blocks. Gain rates in the hypo- or hypermethylated CpG site blocks and each mate in strain-differentially methylated blocks are shown.

Figure 3. Methylation patterns and substitution rates in different tissue types. (A) Comparison of the methylation patterns in Hd-rR: blastulae vs. liver, and testes vs. liver. The vertical and horizontal axes show methylation level. The methylation patterns in HNI are presented in Fig. S5 and are similar to those in these figures. (B) SNP rates in CpG site blocks with three methylation states: hypomethylated in both of the two tissue types, hypermethylated in both, and differentially-methylated between the two tissue types. Significant differences in SNP rates were seen between

tissue-differentially- and hypomethylated regions ($p < 10^{-82}$ by two-proportion z -test, Table S6), and between hypo- and hypermethylated CpG site blocks ($p < 10^{-2170}$, Table S6). **(C)** Dinucleotide substitution rates in CpG site blocks with the three methylation states. The substitution rates of all dinucleotides, except for CC/GG/CG, in tissue-differentially-methylated regions were significantly lower than those in hypomethylated regions ($p < 10^{-3}$ by two-proportion z -test, Table S7A). **(D)** Representative mutation patterns in hypomethylated, hypermethylated, and somatic cell-specific hypomethylated (germ-line-like-specific hypermethylated) regions. Somatic cell-specific hypomethylated regions exhibited the lowest mutation rates.

Figure 4. A working model for higher mutation rate in hypermethylated regions. Deaminated cytosine (U:G mismatch) is repaired by base excision repair (BER), but deaminated 5-methyl-cytosine (T:G mismatch) is corrected by more complicated repair pathways. An alternative mismatch repair system (MMR) might involve low-fidelity DNA polymerase, resulting in the error-prone synthesis of erased gaps.

References

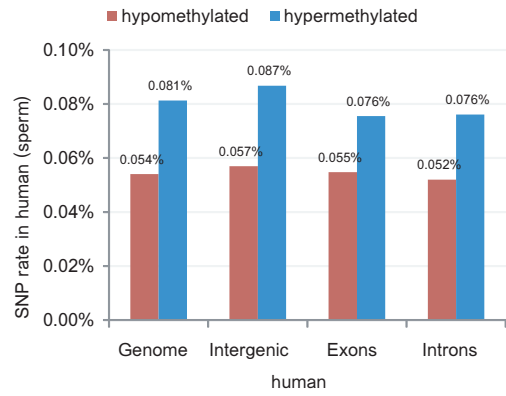
- Burge C, Campbell AM, Karlin S. 1992. Over-Representation and under-Representation of Short Oligonucleotides in DNA-Sequences. *Proceedings of the National Academy of Sciences of the United States of America* **89**(4): 1358-1362.
- Chandler LA, Ghazi H, Jones PA, Boukamp P, Fusenig NE. 1987. Allele-specific methylation of the human c-Ha-ras-1 gene. *Cell* **50**(5): 711-717.
- Cohen NM, Kenigsberg E, Tanay A. 2011. Primate CpG islands are maintained by heterogeneous evolutionary regimes involving minimal selection. *Cell* **145**(5): 773-786.
- Cokus SJ, Feng SH, Zhang XY, Chen ZG, Merriman B, Haudenschild CD, Pradhan S, Nelson SF, Pellegrini M, Jacobsen SE. 2008. Shotgun bisulphite sequencing of the Arabidopsis genome reveals DNA methylation patterning. *Nature* **452**(7184): 215-219.
- Cooper DN, Krawczak M. 1989. Cytosine methylation and the fate of CpG dinucleotides in vertebrate genomes. *Hum Genet* **83**(2): 181-188.

- Coulondre C, Miller JH, Farabaugh PJ, Gilbert W. 1978. Molecular basis of base substitution hotspots in *Escherichia coli*. *Nature* **274**(5673): 775-780.
- Deng J, Shoemaker R, Xie B, Gore A, LeProust EM, Antosiewicz-Bourget J, Egli D, Maherali N, Park IH, Yu J et al. 2009. Targeted bisulfite sequencing reveals changes in DNA methylation associated with nuclear reprogramming. *Nat Biotechnol* **27**(4): 353-360.
- Goll MG, Bestor TH. 2005. Eukaryotic cytosine methyltransferases. *Annual Review of Biochemistry* **74**: 481-514.
- Heijmans BT, Kremer D, Tobi EW, Boomsma DI, Slagboom PE. 2007. Heritable rather than age-related environmental and stochastic factors dominate variation in DNA methylation of the human IGF2/H19 locus. *Hum Mol Genet* **16**(5): 547-554.
- Hellman A, Chess A. 2010. Extensive sequence-influenced DNA methylation polymorphism in the human genome. *Epigenetics Chromatin* **3**(1): 11.
- Hong Y, Winkler C, Schartl M. 1998. Production of medakafish chimeras from a stable embryonic stem cell line. *Proc Natl Acad Sci U S A* **95**(7): 3679-3684.
- International HC. 2003. The International HapMap Project. *Nature* **426**(6968): 789-796.
- Kasahara M, Naruse K, Sasaki S, Nakatani Y, Qu W, Ahsan B, Yamada T, Nagayasu Y, Doi K, Kasai Y et al. 2007. The medaka draft genome and insights into vertebrate genome evolution. *Nature* **447**(7145): 714-719.
- Kerker K, Spadola A, Yuan E, Kosek J, Jiang L, Hod E, Li K, Murty VV, Schupf N, Vilain E et al. 2008. Genomic surveys by methylation-sensitive SNP analysis identify sequence-dependent allele-specific DNA methylation. *Nat Genet* **40**(7): 904-908.
- Lander ES, Linton LM, Birren B, Nusbaum C, Zody MC, Baldwin J, Devon K, Dewar K, Doyle M, FitzHugh W et al. 2001. Initial sequencing and analysis of the human genome. *Nature* **409**(6822): 860-921.
- Li R, Zhu H, Ruan J, Qian W, Fang X, Shi Z, Li Y, Li S, Shan G, Kristiansen K et al. 2010. De novo assembly of human genomes with massively parallel short read sequencing. *Genome Res* **20**(2): 265-272.
- Lindahl T, Nyberg B. 1972. Rate of depurination of native deoxyribonucleic acid. *Biochemistry* **11**(19): 3610-3618.
- Lister R, O'Malley RC, Tonti-Filippini J, Gregory BD, Berry CC, Millar AH, Ecker JR. 2008. Highly integrated single-base resolution maps of the epigenome in *Arabidopsis*. *Cell* **133**(3): 523-536.
- Lister R, Pelizzola M, Dowen RH, Hawkins RD, Hon G, Tonti-Filippini J, Nery JR, Lee L, Ye Z, Ngo QM et al. 2009. Human DNA methylomes at base resolution show widespread epigenomic differences. *Nature* **462**(7271): 315-322.
- Loeb LA, Monnat RJ, Jr. 2008. DNA polymerases and human disease. *Nat Rev Genet* **9**(8): 594-604.
- Meaburn EL, Schalkwyk LC, Mill J. 2010. Allele-specific methylation in the human genome: implications for genetic studies of complex disease. *Epigenetics* **5**(7): 578-582.
- Molaro A, Hodges E, Fang F, Song Q, McCombie WR, Hannon GJ, Smith AD. 2011. Sperm methylation profiles reveal features of epigenetic inheritance and evolution in primates. *Cell* **146**(6): 1029-1041.
- Neddermann P, Gallinari P, Lettieri T, Schmid D, Truong O, Hsuan JJ, Wiebauer K, Jiricny J. 1996. Cloning and expression of human G/T mismatch-specific thymine-DNA glycosylase. *Journal of Biological Chemistry* **271**(22): 12767-12774.
- Ohno S. 1988. Universal rule for coding sequence construction: TA/CG deficiency-TG/CT excess. *Proc Natl Acad Sci U S A* **85**(24): 9630-9634.
- Ossowski S, Schneeberger K, Lucas-Lledo JI, Warthmann N, Clark RM, Shaw RG, Weigel D, Lynch M. 2010. The rate and molecular spectrum of spontaneous mutations in *Arabidopsis thaliana*. *Science* **327**(5961): 92-94.

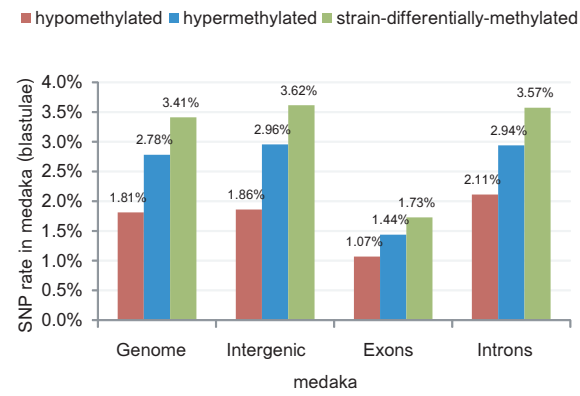
- Sasaki S, Mello CC, Shimada A, Nakatani Y, Hashimoto S, Ogawa M, Matsushima K, Gu SG, Kasahara M, Ahsan B et al. 2009. Chromatin-associated periodicity in genetic variation downstream of transcriptional start sites. *Science* **323**(5912): 401-404.
- Saxonov S, Berg P, Brutlag DL. 2006. A genome-wide analysis of CpG dinucleotides in the human genome distinguishes two distinct classes of promoters. *Proc Natl Acad Sci U S A* **103**(5): 1412-1417.
- Schalkwyk LC, Meaburn EL, Smith R, Dempster EL, Jeffries AR, Davies MN, Plomin R, Mill J. 2010. Allelic skewing of DNA methylation is widespread across the genome. *Am J Hum Genet* **86**(2): 196-212.
- Schilling E, El Chartouni C, Rehli M. 2009. Allele-specific DNA methylation in mouse strains is mainly determined by cis-acting sequences. *Genome Research* **19**(11): 2028-2035.
- Schmitz RJ, Schultz MD, Lewsey MG, O'Malley RC, Urich MA, Libiger O, Schork NJ, Ecker JR. 2011. Transgenerational Epigenetic Instability Is a Source of Novel Methylation Variants. *Science* **334**(6054): 369-373.
- Setiamarga DH, Miya M, Yamanoue Y, Azuma Y, Inoue JG, Ishiguro NB, Mabuchi K, Nishida M. 2009. Divergence time of the two regional medaka populations in Japan as a new time scale for comparative genomics of vertebrates. *Biol Lett* **5**(6): 812-816.
- Shoemaker R, Deng J, Wang W, Zhang K. 2010a. Allele-specific methylation is prevalent and is contributed by CpG-SNPs in the human genome. *Genome Res* **20**(7): 883-889.
- Shoemaker R, Deng J, Wang W, Zhang K. 2010b. Allele-specific methylation is prevalent and is contributed by CpG-SNPs in the human genome. *Genome Research* **20**(7): 883-889.
- Sved J, Bird A. 1990. The expected equilibrium of the CpG dinucleotide in vertebrate genomes under a mutation model. *Proc Natl Acad Sci U S A* **87**(12): 4692-4696.
- Taylor MS, Kai C, Kawai J, Carninci P, Hayashizaki Y, Semple CA. 2006. Heterotachy in mammalian promoter evolution. *PLoS Genet* **2**(4): e30.
- Venter JC Adams MD Myers EW Li PW Mural RJ Sutton GG Smith HO Yandell M Evans CA Holt RA et al. 2001. The sequence of the human genome. *Science* **291**(5507): 1304-1351.
- Weber M, Hellmann I, Stadler MB, Ramos L, Paabo S, Rebhan M, Schubeler D. 2007. Distribution, silencing potential and evolutionary impact of promoter DNA methylation in the human genome. *Nat Genet* **39**(4): 457-466.
- Yamada Y, Watanabe H, Miura F, Soejima H, Uchiyama M, Iwasaka T, Mukai T, Sakaki Y, Ito T. 2004. A comprehensive analysis of allelic methylation status of CpG islands on human chromosome 21q. *Genome Res* **14**(2): 247-266.
- Yoon JH, Iwai S, O'Connor TR, Pfeifer GP. 2003. Human thymine DNA glycosylase (TDG) and methyl-CpG-binding protein 4 (MBD4) excise thymine glycol (Tg) from a Tg:G mismatch. *Nucleic Acids Res* **31**(18): 5399-5404.
- Zhang Y, Rohde C, Tierling S, Jurkowski TP, Bock C, Santacruz D, Ragozin S, Reinhardt R, Groth M, Walter J et al. 2009. DNA methylation analysis of chromosome 21 gene promoters at single base pair and single allele resolution. *PLoS Genet* **5**(3): e1000438.

Figure 1

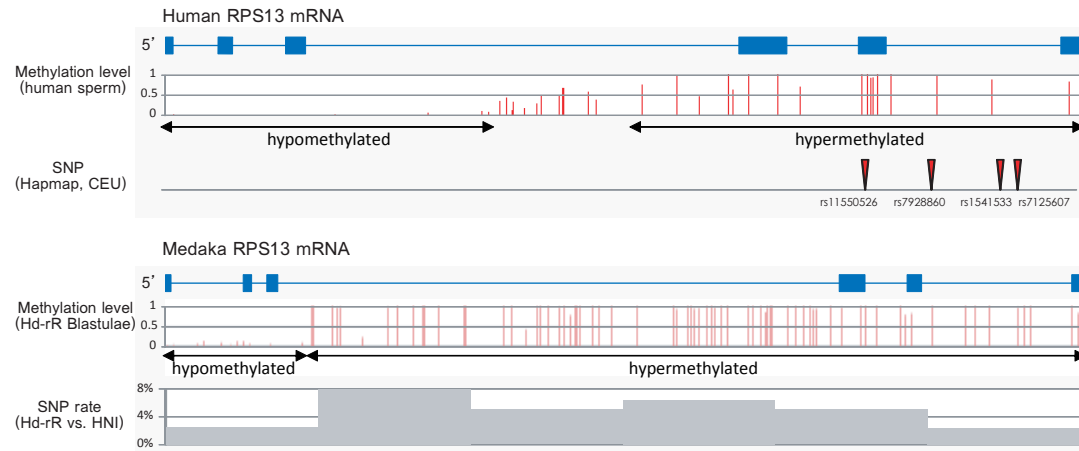
A



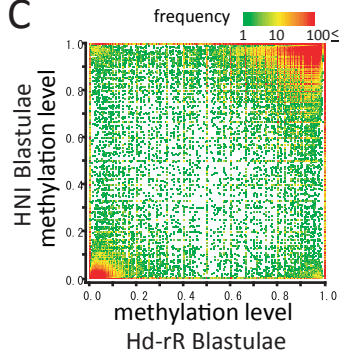
F



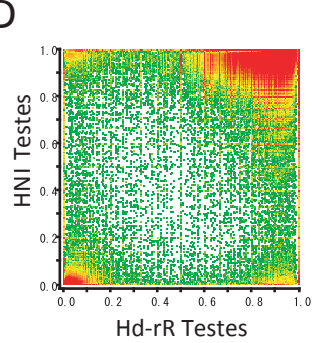
B



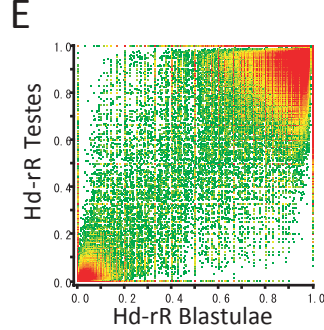
C



D



E



G

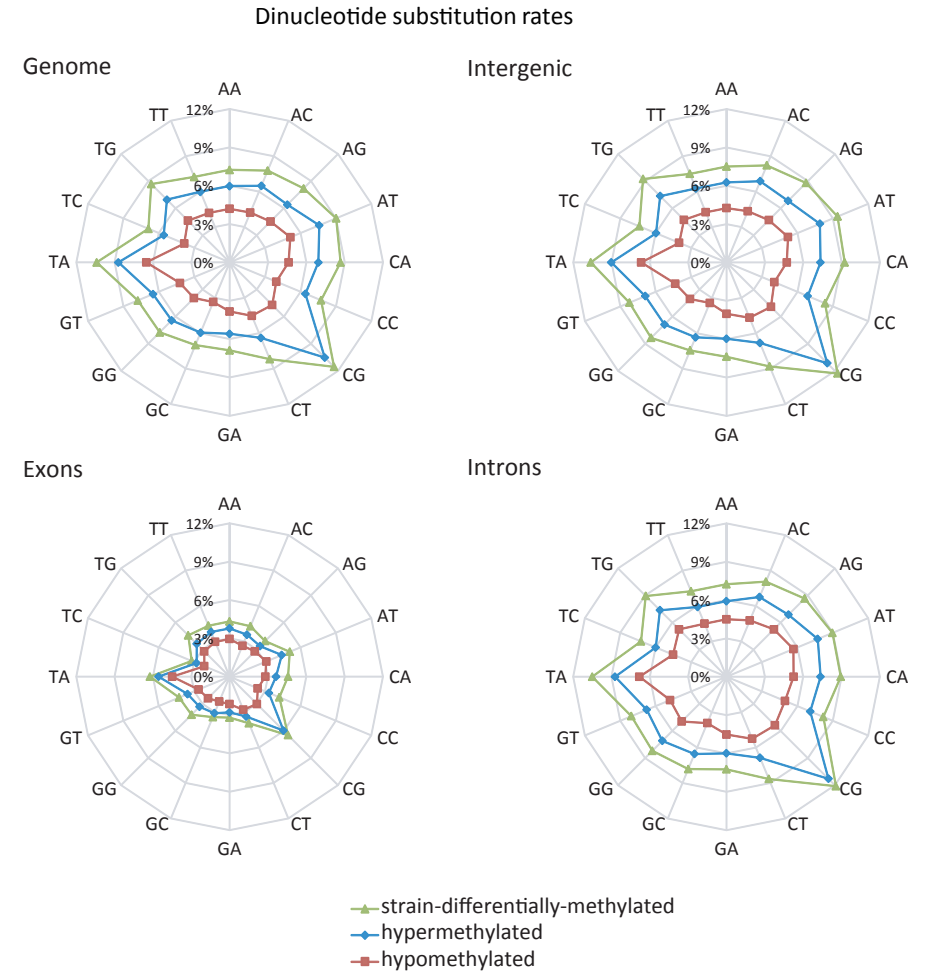
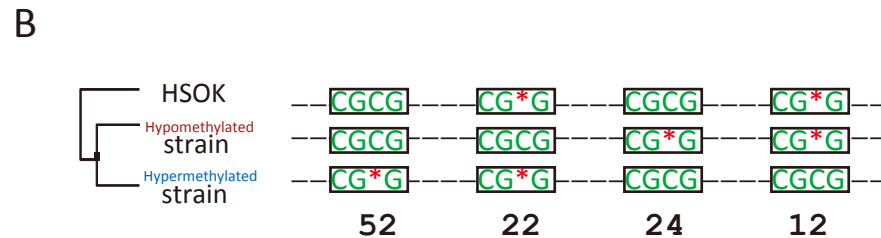
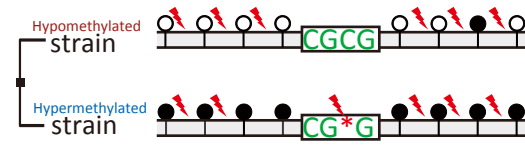
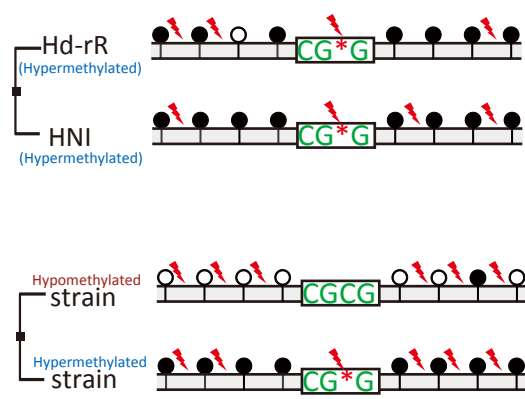
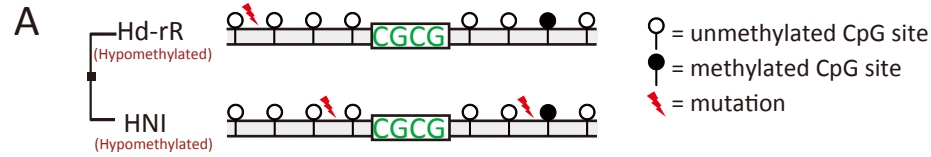


Figure 2



C
Rates of dinucleotide-gaining in CpG site blocks

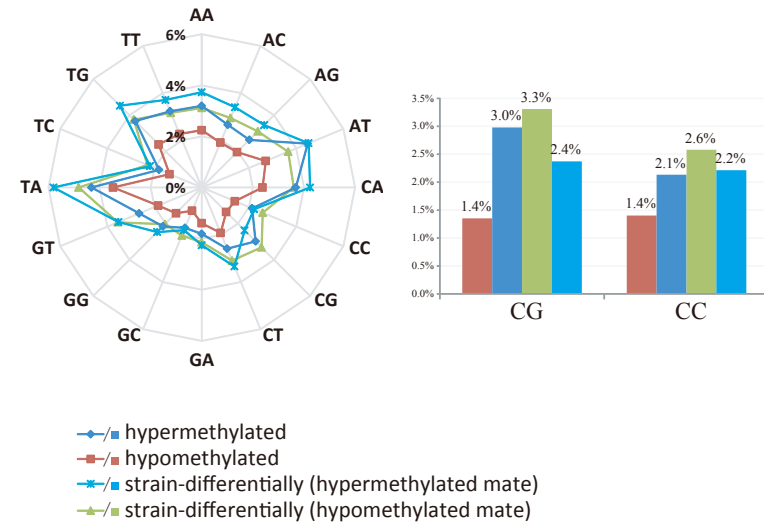


Figure 3

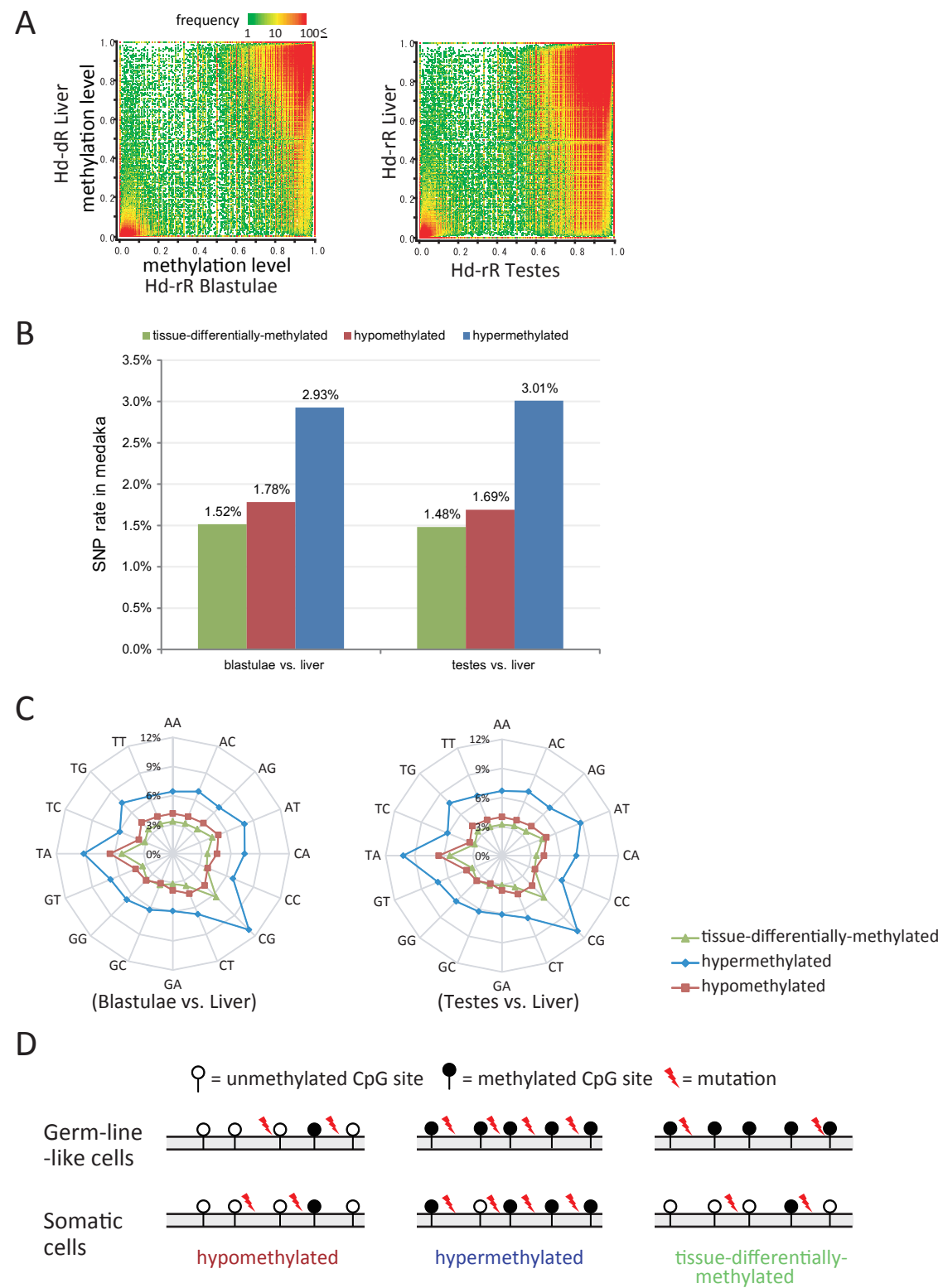


Figure 4

